*Highlights on Spanish Astrophysics IX, Proceedings of the XII Scientific Meeting of the Spanish Astronomical Society held on July 18 – 22, 2016, in Bilbao, Spain. S. Arribas, A. Alonso-Herrero, F. Figueras, C. Hernández-Monteagudo, A. Sánchez-Lavega, S. Pérez-Hoyos (eds.)*

# A pilot search for mm-RRLs in pre-Planetary Nebulae

**C. Sánchez Contreras[1], A. Báez-Rubio[1,2], J. Alcolea[3], V. Bujarrabal[3], and J. Martín-Pintado[1]**

[1] Centro de Astrobiología (CSIC-INTA). ESAC campus, Camino Bajo del Castillo s/n, Urb. Villafranca del Castillo, E-28691 Villanueva de la Cañada, Madrid, Spain
[2] Instituto de Astronomía, Universidad Nacional Autónoma de México, Mexico
[3] Observatorio Astronómico Nacional (IGN), Madrid, Spain

## Abstract

We carried out pilot search for radio recombination line (RRL) emission at millimeter wavelengths in a small sample of pre-Planetary Nebulae (pPNe) and young PNe (yPNe) with emerging central ionized winds. RRLs at mm-wavelengths are excellent probes of the dense inner (<150 au) regions of these objects, where the yet unknown agents for PN-shaping operate, and which are usually heavily obscured at shorter wavelengths by optically thick circumstellar dust shells. We detect mm-RRLs in three objects: CRL 618, MWC 922, and M 2-9. We present the results from detailed line + continuum non-LTE 3D radiative transfer models for these targets, which enables constraning the structure, kinematics, and physical conditions (electron temperature and density) of their ionized cores. Amongst other parameters, we derive mass-loss rates of $\dot{M}_{\rm pAGB} \approx 10^{-6}$-$10^{-7}\,M_\odot$ yr$^{-1}$, which are significantly higher than the values adopted by stellar evolution models currently in use.

## 1 Introduction

The yet unknown physical mechanisms responsible for the onset of asphericity and polar acceleration in Planetary Nebulae (PNe) are active in the early stages of the evolution beyond the AGB. Therefore, pre-PNe (pPNe) and young PNe (yPNe) hold the key for understanding the complex and fast (∼1000 yr) evolution from the AGB toward the PN phase. Studies of pPNe support the idea that the multiple lobes and high-velocities observed are produced by the impact of collimated fast winds (CFWs or *jets*) on the spherical and slowly expanding circumstellar envelopes (CSEs) formed in the previous AGB phase (see, e.g., the review paper by [1]). However, this jet+'AGB CSE' interaction scenario remains unconfirmed by direct

Table 1: Sample of pPNe/yPNe, with $T_{\rm eff}$∼20,000-40,000 K central stars, in our pilot study. The continuum flux measured by us near 2.7 mm and 1.3 mm is given.

| Source name | RA(J2000) ($^{\rm h}$ $^{\rm m}$ $^{\rm s}$) | Dec(J2000) ($^{\rm o}$ ' ") | Continuum (mJy) 2.7 mm | 1.3 mm | Distance (kpc) | Luminosity ($10^3$ $L_\odot$) |
|---|---|---|---|---|---|---|
| *RRLs detections* | | | | | | |
| CRL 618 | 04:42:53.64 | +36:06:53.4 | 2395(±17) | 2670(±50) | 0.9 | 8.5 |
| M 2-9 | 17:05:37.96 | −10:08:32.5 | 121(±3) | 180(±10) | 0.65,1.3[a] | 0.7,3.0[a] |
| MWC 922 | 18:21:15.91 | −13:01:27.1 | 109(±2) | 203(±5) | 1.7,3.0[a] | 18,59[a] |
| *RRLs non-detections* | | | | | | |
| He 3-1475 | 17:45:14.19 | −17:56:46.9 | 6(±2) | 31(±10) | 5 | 9 |
| M 1-91 | 19:32:57.69 | +26:52:43.1 | 12(±1) | 23(±3) | 2.1 | 0.3 |
| M 1-92 | 19:36:18.90 | +29:32:49.9 | 18(±2) | 86(±2) | 2.5 | 10 |
| IRAS 20462+3416 | 20:48:16.63 | +34:27:24.3 | 6(±2) | 16(±3) | 3.5 | 0.8 |
| M 2-56 | 23:56:36.38 | +70:48:17.9 | 6(±1) | 39(±4) | 2.1 | 5.5 |

[a]Uncertain distance/luminosity, two possible values are given.

characterization of the post-AGB jets themselves, and of the central nebular regions from where these would be launched (within ∼few×100 au). Studying these central regions is difficult due to their small (sub-arcsec) angular sizes and, most importantly, because they are usually heavily obscured by optically thick circumstellar dust shells.

The central, just emerging ionized cores of pPNe/yPNe can be traced by radio recombination line (RRL) emission with the important advantage that dust extinction effects are minimal. To date, mm- but mainly cm-wavelength RRLs studies have been carried out for some of the best known and most luminous evolved PNe. However, this field remains largely unexplored for pPNe/yPNe, where central ionized regions are in an early stage of development inmediately after their central stars start ionizing their surroundings (typically when they reach a B-type spectral clasification).

## 2 Observations and results

Observations of the lines H30$\alpha$, H31$\alpha$, H39$\alpha$, H41$\alpha$, H48$\beta$, H49$\beta$, H51$\beta$, and H55$\gamma$ at ∼1 and ∼3 mm have been performed with the IRAM 30 m radiotelescope (Pico Veleta, Granada, Spain) towards a sample of eight pPNe/yPNe with H$\alpha$ and free-free radiocontinuum emission from their compact ionized cores (Table 1). Spectra were taken using the new generation heterodyne Eight MIxer Receiver (EMIR) in two observational campaigns in June/July and September 2015. More details are given in Sánchez Contreras et al. (in preparation - SC+17).

In all targets, we detect mm-continuum emission (Table 1), which is a mixture of thermal dust and free-free emission. To our knowledge, MWC 922, M 1-91, IRAS 20462+3416, and M 2-56 represent first mm-continuum emission detections. We find that the mm-to-cm continuum follows a $S_\nu \propto \nu^{[0.6:1.6]}$ power-law distribution consistent with optically thick ionized winds with steep density gradients. Flux-density variations and changes of the spectral

index with time are inferred for some targets (for example, the well known pPN CRL 618, which shows abrupt and impredictable flux changes that most likely denote alterations in the activity and/or physical conditions of the post-AGB wind at its core, see e.g.[7]).

We detected mm-RRLs in three objects, CRL 618, MWC 922, and M 2-9, which are the strongest mm-continuum emitters (Fig. 1). The line flux, full width at half maximum (FWHM) and centroid of the different transitions (derived from gaussian-profile fitting) are shown in Fig. 2.

Prior to our work, RRLs have only been sought and detected in the mm-wavelength range (H41$\alpha$, H35$\alpha$, and H30$\alpha$) towards one pPN, CRL 618 [5]. We detect now a total of eight Hydrogen recombination lines ($\alpha$, $\beta$, and $\gamma$) together with Helium and Carbon $\alpha$-transitions. The mm-RRLs profiles are partially blended with some of the many molecular transitions, with composite emission+absorption profiles, that crowd the submm/mm spectrum of this object [6]. We find significant changes in the spectral profiles and total fluxes of the H41$\alpha$ and H30$\alpha$ lines of CRL 618 relative to the observations performed in 1987 by [5], consistent with a varying stellar wind. In particular, these RRLs are now a factor $\sim$2-3 more intense and $\sim$20-60% broader than $\sim$30 years ago.

In M 9-2, weak emission from the H30$\alpha$ and H39$\alpha$ lines and, tentatively, from the H31$\alpha$ and H41$\alpha$ transitions is detected. In MWC 922, we detect the four Hn$\alpha$ transtions sought in this work and also the weaker H48$\beta$ and H49$\beta$ lines. In contrast to CRL 618 and M 2-9, in this source, there is an evident change from Hn$\alpha$ single-peaked profiles near 3mm to double-peaked profiles near 1 mm. The two-horned profiles, observed to date only in a handful of sources (e.g. the ultra-compact HII region MWC 349A – [2]), indicate maser amplification of the emission. This is corroborated by the very steep dependency of the mm-RRLs strength with frequency observed in MWC 922, which is a sign of emission under non-LTE conditions.

There are some general results about the kinematics of the ionized cores of our targets that can be readily deduced from the RRLs profiles (Figs.1 and 2). The linewdiths of the H$\alpha$-transitions range between FWHM $\sim$30 and 50 km s$^{-1}$ and, thus, are larger than expected from thermal motions alone (e.g. the sound speed is $c_s\sim$13 km s$^{-1}$ for ionized gas with an average electron temperature of $T_{\rm e}\approx$10,000 K) and indicate macroscopic ordered motions at moderate speeds of $\approx$10-30 km s$^{-1}$.

The Hn$\alpha$ linewidth increases with increasing quantum number $n$ (i.e. decreasing line frequency) in CRL 618 and (tentatively) M 2-9, but the opposite behavior is found for MWC 922. The higher-$n$ transitions (at lower frequencies) trace more tenuous regions than lower-$n$ lines (at higher frequencies and, thus, less optically thin). Therefore, assuming that the density in the ionized region falls off with the radial distance to the center ($r$), the observed trend suggests that $V_{\rm exp}$ increases with the distance to the star, consistent with an expanding wind, in CRL 618 and M 2-9. In the case of MWC 922, the spectra seem more consistent with a rotating disk, where one expects the rotation speed to decrease with $r$.

## 3 Non-LTE radiative transfer modeling

In order to constrain the structure, physical conditions, and kinematics of the emerging ionized regions of CRL 618, MWC 922 and M 2-9, we have modeled the free-free continuum

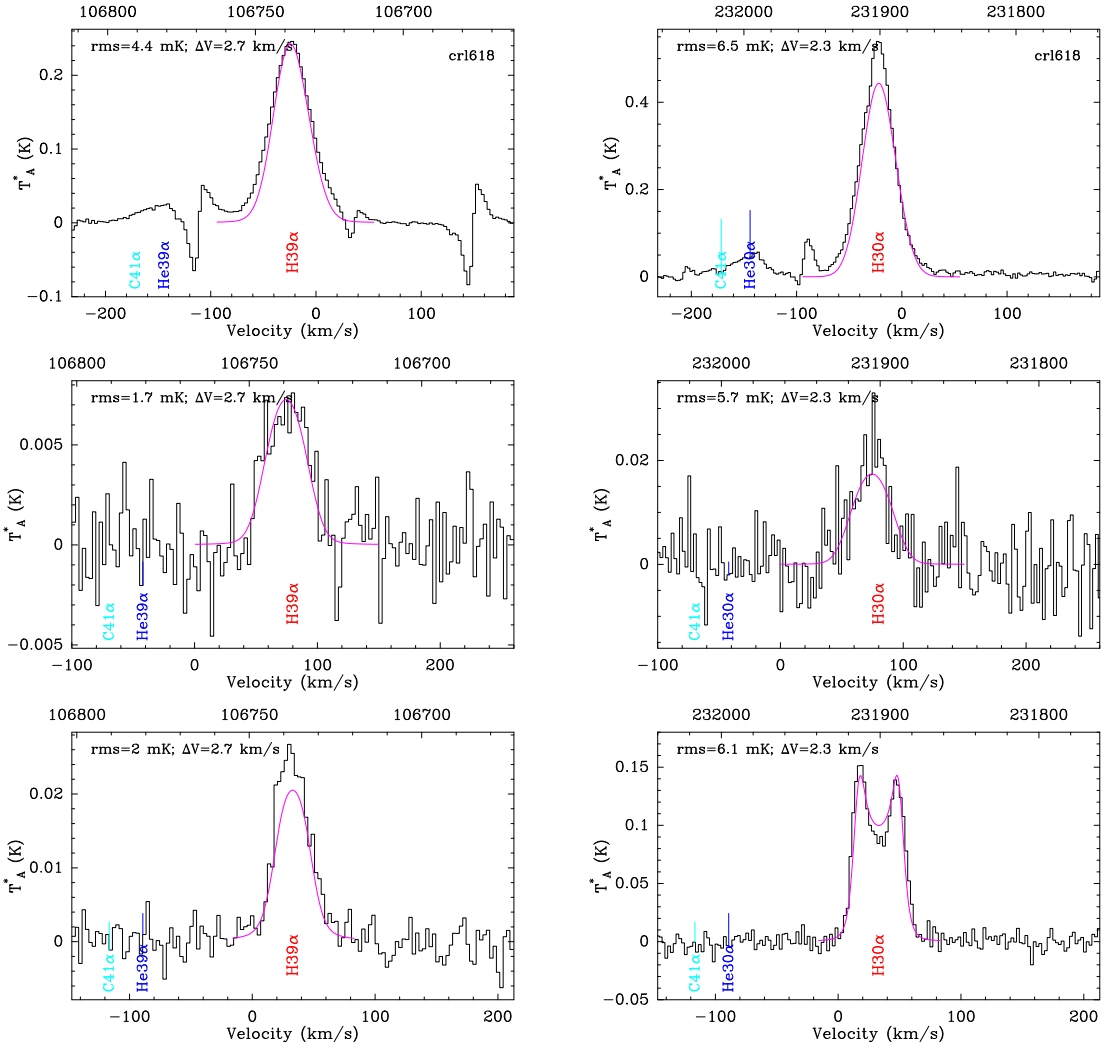


Figure 1: Some of the recombination lines at ∼3mm (left) and ∼1 mm (right) detected towards CRL 618, M 2-9, and MWC 922 (from top to bottom); synthetic line profiles from our 3D non-LTE radiative transfer model are overimposed (pink line).

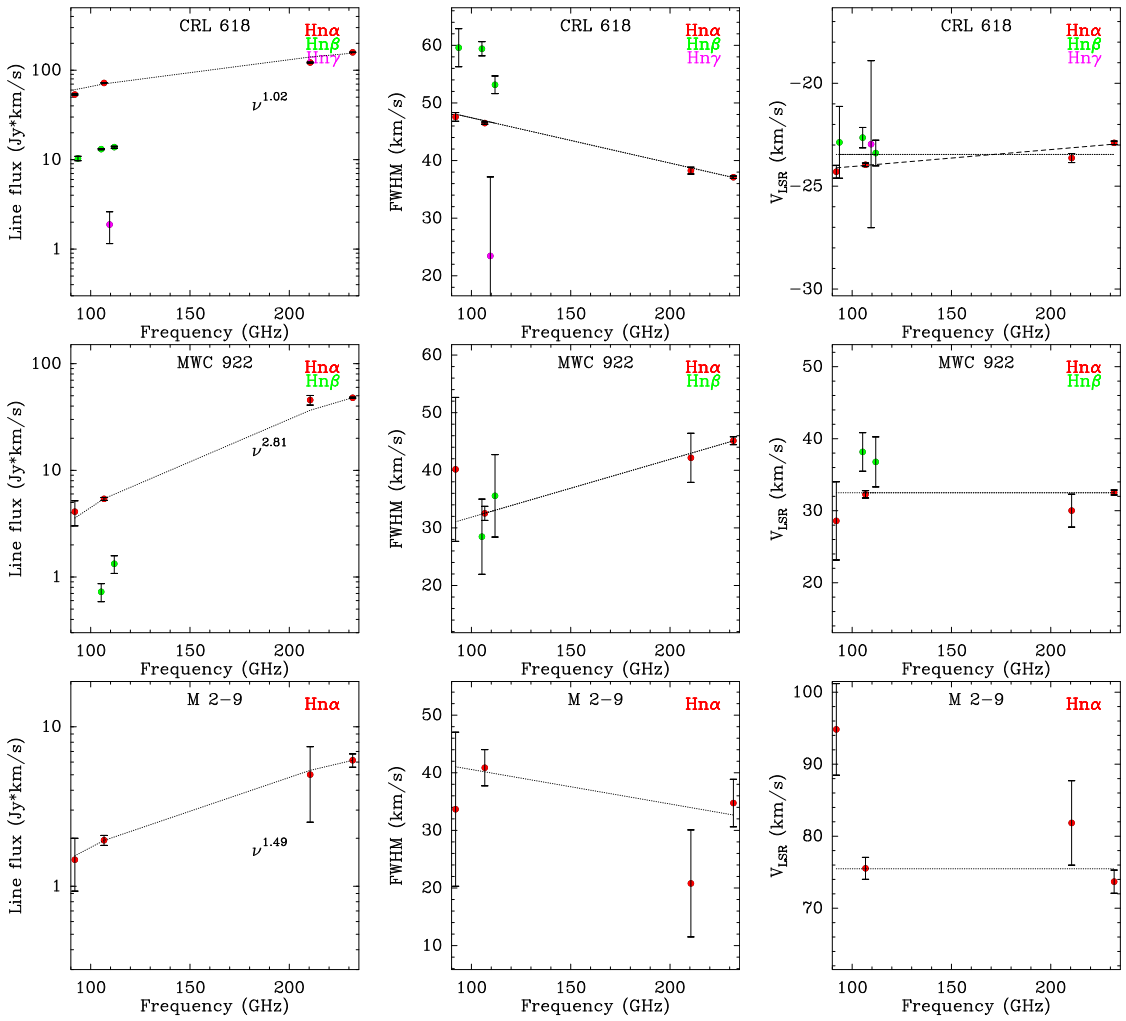


Figure 2: RRLs parameters of CRL 618, MWC 922, and M 2-9 (from top to bottom).

and mm-RRLs observed in these targets using the LTE and non-LTE 3D radiative transfer code MORELI (MOdel for REcombination LInes, [2]). The geometry of the ionized region, as well as the electron density, electron temperature and the velocity field, are the main input parameters of our model. The detailed model assumptions and results are presented in SC+17. A summary is provided here.

The RRLs and continuum data for CRL 618 are well reproduced assuming an isothermal stellar wind represented by a cylinder of ionized gas with a central cavity around the star, constant electron temperature ($T_{\rm e}$∼17,000 K) and an inverse-square density profile. The electron densities range between $n_{\rm e}$ ∼3×10$^7$ and 5×10$^6$ cm$^{-3}$, in the mm-RRLs/continuum emitting region, ∼45-100 au, consistent with an equivalent isotropic mass-loss rate of $\dot{M}_{\rm pAGB}$∼[6-9]×10$^{-6}$ $M_\odot$ yr$^{-1}$. From the observed profiles, and taking into account that the 1 mm and 3 mm lines arise in neirghboring layers, probably only ≈10 au apart from each other, we

deduce that there must be a steep rise of the velocity at these small spatial scales, from $V_{\rm exp}$∼7-12 km s$^{-1}$ at the innermost regions of the wind (probably near 40-60 au) to $V_{\rm exp}$∼20-25 km s$^{-1}$ near the outer boundary of the modeled region (∼70-90 au).

MWC 922 has been modeled adopting a composite 'rotating disk + ouflow' structure with $T_{\rm e}$∼6000-20,000K. The kinematics of the disk, where the H30$\alpha$-maser spike emission mainly arises (within $r$∼35-55au), is consitent with keplerian rotation around a ∼5-10$M_{\odot}$ central object. The ionized outflow, which may represent a stellar wind or gas photoevaporating from the rotating disk, is expanding at ∼10 km s$^{-1}$ and has densities consistent with an equivalent isotropic mass-loss rate of ∼[2-6]×10$^{-6}$ $M_{\odot}$ yr$^{-1}$.

M 2-9 has been modeled adopting an isothermal ($T_{\rm e}$∼9,000-10,000 K) spherical wind expanding at $V_{\rm exp}$∼20km s$^{-1}$ with $\dot{M}_{\rm pAGB}$∼[2-3]×10$^{-7}$$M_{\odot}$ yr$^{-1}$. We have found a significant difference between the centroids of the mm-RRLs, $V_{\rm LSR}$=75±2km s$^{-1}$, and those of the CO $J$=2–1 transitions. The latter trace two major mass-loss events that happened ∼1500 and ∼900 years ago, lasting only <40 yr (each) and leading to the formation of two thin equatorial rings in expansion [4]. Our mm-RRLs trace a distinct mass outburst that has happened very recently as the mass-lossing star orbits around a companion.

## 4 Summary

We have performed mm-RRLs observations to study the stucture, physical conditions and kinematics of the, up to date inscrutable, ionized cores of pPNe/yPNe. Our analysis, which includes line and continuum radiative transfer modelling, has allowed us to characterize the relatively dense, inner (< 150 au) ionized regions of CRL 618, M 2-9, and MWC 922: we derive electron temperatures $T_{\rm e}$∼6000-18,000 K, mean densities of $n_{\rm e}$∼ 10$^{[6-8]}$ cm$^{-3}$, density gradients of $n_{\rm e}$∝ $r^{-\alpha_n}$ with $\alpha_n$=[2.0:2.4], and motions with velocities of ∼10-30 km s$^{-1}$. Considering their expansion velocities and small extent, these inner regions probe very recent mass ejections events happened less than ∼15-20 yr. Post-AGB mass-loss remains very poorly known even when it is key to understanding the physics mediating the AGB-to-PN evolution. From our study, we derive typical mass-loss rates of $\dot{M}_{\rm pAGB}$≈10$^{-7}$-10$^{-6}$ $M_{\odot}$ yr$^{-1}$, which are significantly larger than those adopted for similar objects by post-AGB evolutionary models currently in use (e.g. [3]).

## References

[1] Balick, B., & Frank, A. 2002, ARA&A, 40, 439

[2] Báez-Rubio, A., Martín-Pintado, J., Thum, C., & Planesas, P. 2013, A&A, 553, A45

[3] Bloecker, T. 1995, A&A, 299, 755

[4] Castro-Carrizo, A., Neri, R., Bujarrabal, V., et al. 2012, A&A, 545, A1

[5] Martin-Pintado, J., Bujarrabal, V., Bachiller, R., et al. 1988, A&A, 197, L15

[6] Pardo, J.R., Cernicharo, J., Goicoechea, J.R., et al. 2007, ApJ, 661, 250

[7] Sánchez Contreras, C., Bujarrabal, V., Castro-Carrizo, A., et al. 2004, ApJ, 617, 1142